Desalination and Water Treatment
www.deswater.com
doi: 10.5004/dwt.2023.29363

289 (2023) 145–154
March

Single and simultaneous adsorption of inorganic and organic pollutants by NH_4Cl-induced activated carbon produced: isotherm and kinetic studies

Ahmad Alahabadi[a], Mohammad Hossien Saghi[a], Atefeh Dehnabi[a], Forough Riahimanesh[a,b,*]

[a]*Department of Environmental Health, School of Public Health, Sabzevar University of Medical Sciences, Sabzevar, Iran, emails: chem.riahi@gmail.com (F. Riahimanesh), ahmad_health@yahoo.com (A. Alahabadi), saghi9@gmail.com (M.H. Saghi), atefehdehnabi@gmail.com (A. Dehnabi)*
[b]*Cellular and Molecular Research Center, Department of Environmental Health, School of Public Health, Sabzevar University of Medical Sciences, Sabzevar, Iran*

Received 23 July 2022; Accepted 18 January 2023

ABSTRACT

The simultaneous removal of heavy metal and dye as two dangerous environmental pollutants is a challenge for the treatment of industrial wastewater. This work investigates the performance of NH_4Cl-induced activated carbon prepared from sycamore wood (NACSW) for the single and simultaneous removal of Reactive Orange P3R (RO P3R) and chromium(VI). These results indicated NACSW could be a favorable adsorbent for the simultaneous removal of the dye and heavy metal. The structure of prepared activated carbon was evaluated using Fourier-transform infrared spectroscopy, scanning electron microscopy, Brunauer–Emmett–Teller, etc analyses. The effects of solution pH, pollutants dosage, NACSW dosage, and contact time on the removal performances in separate and simultaneous samples were investigated. The equilibrium isotherms model is consistent with the Temkin model. The kinetics results demonstrated that RO P3R and Cr adsorption were followed by the Elovich kinetic model. The removal percentage in single and simultaneous states was not significantly different, indicating that the sorption sites of dye and chromium on NACSW were various.

Keywords: Simultaneous removal; Activated carbon; Chromium; Textile dyes

1. Introduction

Recently, with releasing toxic contaminants in water resources, severe environmental problems have been caused by the proliferation of industries and growth in the production of different types of consumer goods [1–3]. Unfortunately, containing both inorganic and organic pollutants, most of the industrial wastes could be transported into wastewaters [4]. Having severe effects on human health even at trace concentrations, heavy metals could lead to severe environmental problems. chromium (Cr) has many applications in industry, including pigment manufacturing, leather tanning, textile processing, oil refining, and electroplating. Either indirectly or directly discharged, wastewaters containing chromium may cause severe pollution [5–9]. Existing chromium compounds in the environment are of two types: Cr(III) (trivalent chromium) and Cr(VI) (hexavalent chromium). Drinking water could be contaminated because of incorrect disposal of wastewaters containing chromium, especially hexavalent chromium [10,11]. An aqueous environment contaminated with chromium could intoxicate aquatic organisms and human beings [12,13]. Exposure of human skin to chromium(VI)-containing wastewater for a longer period could lead to eczema and dermatitis. Also, breathing hexavalent chromium may cause nosebleed, running nose, sneezing, ulcer, carcinogenicity, affected circulatory system, mutagenicity, and nephrogenic damage [14,15].

* Corresponding author.

Drinking chromium(VI)-containing water was found to be associated with carcinogenicity [16].

In recent years, a surge of demand has occurred in the textile production industry. Annually, 700,000 tons of synthetic dyes are produced, with more than 100,000 commercially available dyes worldwide [17–19]. Water plays an essential role in textile processing. In the medium-sized textile industry, 1.6 million L of water are daily required for fabric processing [20–22]. As an essential component in the textile and chemical industry, textile dyes represent approximately 70% of the dye market [23]. Water supplies containing textile dyes may cause severe problems including blurred vision, diarrhea, cancer, nausea, irritated skin, changes in cellular functioning, and allergic reactions [21,24]. Besides, insufficient light penetration slows down the self-purification of water streams. Therefore, the removal of dye from potable water is essentially recommended [25,26]. Reactive Orange P3R (RO P3R) as textile dyes are widely used in Iranian textile industry.

To deal with contaminants, several methods have been used including oxidation, adsorption, ion exchange, reverse osmosis, electrochemical purification, and biosorption [27,28]. Being an efficient and cost-effective method, adsorption is considered the most effective method for wastewater treatment [29–31]. During adsorption process, because of electrostatic and hydrophobic interaction between adsorbent and adsorbate, a contaminant adheres to an adsorbent. Many different materials are used as adsorbents including biomasses, activated carbon, biochars, silica, carbon nanotubes, and polymers [32–36]. Although many adsorbents exist, a cost-effective and practical adsorption process depends only on using easily accessible and low-cost materials [37]. Having a porous structure, high surface area, and considerable efficiency in removing inorganic and organic pollutants, activated carbons (AC) are widely used in drinking water treatment. Also, higher adsorption capacity and abundant surface functional groups, along with the above-mentioned features have caused to draw many researchers' attention toward activated carbons [38–41]. Nonetheless, given the high production cost of commercial AC, agricultural wastes are found to be viable feedstock alternatives to produce affordable AC [37,42].

This study aimed to investigate the potential of NH_4Cl-assisted activated carbon prepared from sycamore wood (NACSW). The originality and importance of the present study is that it examines simultaneous and single adsorption of reactive dye and chromium to understand the effect of simultaneous removal on the amount of adsorption in NACSW, as well as the interaction between the activated carbon with pollutants and pollutants together. In this research, the effect of solution pH, adsorbent dosage, concentrations of pollutants, and contact time on the adsorption of reactive dye and chromium were investigated. Isotherm and kinetic of activated carbon and pollutant adsorption were also evaluated.

2. Materials and methods

2.1. Materials

All AR-grade chemicals were applied. $K_2Cr_2O_7$, NH_4Cl, NaOH, and HCl were purchased from Merck & Co. A stock solution of chromium (1,000 mg/L) was prepared from $K_2Cr_2O_7$ salt. By adequate dilution of the stock solutions, working solutions with desired concentrations were prepared. To prepare the industrial reactive dye was used the product of Hamedan Alvan Sabet Co., Iran. Using dilute solutions of NaOH and HCl, the pH of test solutions was set to the intended value. In all experiments, deionized water was applied. Activated carbon was prepared according to a multi-step process, commonly used in the author's research group [43]. To remove impurities, the sycamore wood was first washed several times with deionized water. Afterward, it was oven at 100°C for 1 d. The wood pieces (under N_2 gas stream) were carbonized at 700°C for 1 h. The carbonized woods were then steeped in the ammonium chloride solution (2 wt.%) and were shaken for 2 h. The char was oven-dried at 110°C for 24 h and activated under N_2 atmosphere by oven-heating for 2 h at 800°C.

2.2. Adsorption experiments

A stirred (100 rpm) glass reactor was used to perform batch adsorption experiments. Prior to adding heavy metal and dye solution, the adsorbent was added to each flask in different amounts. By using a pH meter (Metrohm 827), the adsorbent pH was adjusted at the desired level, and the suspension was mixed at contact time. By using a 0.2 μm pore size cellulose acetate filter, the suspension was filtered upon ending the predetermined mixing time. An analysis was also conducted on filtrate for residual pollutants. The concentration of Cr and reactive dye was measured using Atomic Absorption Spectroscopy AA-7000 Series – Shimadzu and Hach DR 5000 UV-Vis Spectrophotometer, respectively. To ensure reproducibility of results, all experiments were thrice conducted, and each evaluation was represented by mean of these three measurements. Using the following equation, removal efficiency (RE) and adsorption capacity (q_t) were calculated [Eqs. (1) and (2)]:

$$\mathrm{RE}\% = \frac{C_0 - C_t}{C_0} \times 100 \tag{1}$$

$$q_t = \frac{C_0 - C_t}{m} \times V \tag{2}$$

where C_0 indicates pollutant concentration at initial and C_t at time t of contact time. V and m are volume of solution and the mass of adsorbent, respectively.

2.2.1. Adsorption isotherm

By adding 0.04 gr NACSW to Erlenmeyer flasks, containing 100 mL of various concentrations (50–500 mg/L) with a pH of 4. Adsorption equilibrium onto prepared activated carbon was evaluated. Then, flasks were stirred at 25°C for 6 h, after which the suspension was analyzed. Also, using isotherm models of Freundlich, Langmuir, and Temkin for simultaneous and separate dye and chromium adsorption equilibrium onto prepared AC were then modelled.

The Langmuir isotherm could evaluate the highest removal capacity of the adsorbent which is associated with

monolayer surface of the adsorbent. What follows deals [Eq. (3)] with the non-linear equation of Langmuir:

$$q_e = \frac{q_m K_L C_e}{1 + K_L C_e} \tag{3}$$

where K_L (L/mg) is constant of Langmuir and relevant to the energy of adsorption, q_e is the amount of polluter that can be adsorbed by NACSW at equilibrium (mg/g), q_m (mg/g) is the theoretical highest adsorption capacity and C_e (mg/L) is the contaminant concentration at equilibrium.

The Freundlich isotherm is generally used to determine the adsorption intensity of surfaces of adsorbate with uneven energy distribution. What follows is the Freundlich nonlinearized equation [Eq. (4)].

$$q_e = K_F C_e^{1/n} \tag{4}$$

where n and K_F, are constants from the Freundlich equation.

The Temkin isotherm states that reducing the heat of adsorption of all the molecules in the layer followed the linear trend rather than a logarithmic curve. The non-linear Temkin isotherm is:

$$q_e = B \ln\left(K_t C_e\right) \tag{5}$$

where K_t and B represent the Temkin constants.

2.2.2. Adsorption kinetics models

The adsorption kinetic model is studied by analyzing experimental data obtained from examining the time effect on the removal percent. Investigation of kinetic model is helpful in providing worthwhile info about its mechanism and determining overall rate of the adsorption process. In the present study, the kinetic was checked with different kinetic models of pseudo-first-order, pseudo-second-order, and Elovich.

The pseudo-first-order kinetic model is as follows:

$$q_t = q_e\left(1 + \exp\left(-k_1 t\right)\right) \tag{6}$$

The q_e and k_1 can be obtained through the plot of q_t vs. t.

Being usually used to explain adsorption dynamics, the pseudo-second-order is as follows:

$$q_e = \frac{q_t^2 k_2 t}{q_e k_2 t + 1} \tag{7}$$

Elovich equation kinetic has been used for describing the mechanism of substance adsorption:

$$q_t = \frac{1}{\beta}\left(1 + \alpha\beta t\right) \tag{8}$$

By the plot of q_t vs. t. α, and β can be calculated.

3. Results and discussion

The surface morphology of the NACSW is key feature that affects the absorption rate of pollutants. Scanning electron microscopy (SEM) analyzed the morphology and surface of activated carbon from sycamore wood. The long parallel, well-developed channels, and smooth surface were observed, as shown in Fig. 1. Jiang et al. [44] reported similar SEM microstructures of activated carbon prepared from lignocellulosic biomass prepared via direct activation route.

The Fourier-transform infrared spectroscopy (FTIR) spectrum of AC (range of wavenumber of 4,000–400 cm^{-1}) can be observed in Fig. 2. The presence of various characteristic bands on the surface of AC was detected by FTIR that the most important of which are as follows. An absorption band at 3,433 cm^{-1} is representative of hydroxyl functional groups. The peak at 2,929 cm^{-1} is attributed to the aliphatic stretching of C–H. The peaks about 1,634 are ascribed to the C=O groups in the carboxylic groups. C–O groups' band identified at proximately 1,091 cm^{-1}.

Textural characteristics of AC are given in Table 1.

3.1. Effect of pH on removal

The efficacy of pH on the removal of the separate and simultaneous sample Reactive Orange P3R and chromium by NACSW was investigated. The removal rates under experimental conditions (50 mL of 25 mg/L solutions of synthetic wastewater at 15 min) in pHs between 2 and 9 were

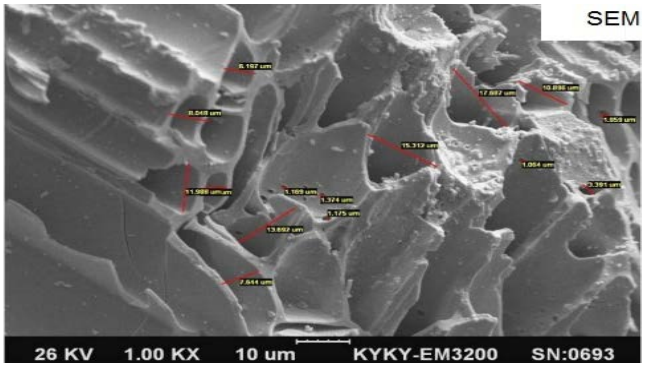

Fig. 1. Scanning electron microscopy images micrographs of the NACSW.

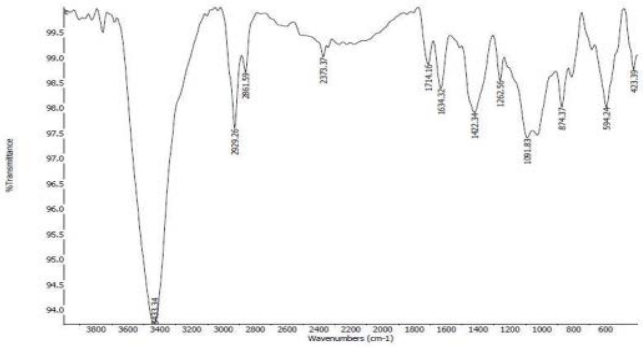

Fig. 2. Fourier-transform infrared spectra of NACSW.

examined. The results demonstrate that pH is significant to the removal of this contaminant.

The results showed (Fig. 3) that the percentage of RO P3R adsorption at pH 2 to 4 in single and simultaneous adsorption remains stable at 84% and 70%, respectively. The removal percentage of dye decreases with increasing pH from 4.0 to 9.0, and in pH = 9 the removal percentage was 20% (single removal) and 12% (simultaneous removal). In pH < pH_{PZC} (7.5), the removal of dye (%) by AC increased due to the electrostatic attraction between the molecules of dye with negative charge and the positive charge of the adsorbent surface [45]. At pHs higher than pH_{PZC}, the percentage of removal dye is drastically reduced as the electrostatic repulsion force between the negatively charged ions of the anionic dye and the adsorbent. Similar results were also found by Calvete et al. [46] and Abdulhameed et al. [47] in the removal of Reactive Orange 16 dye. Eslek Koyuncu et al. [48] have reported that while the pH is raised from 1 to 7, the AV 90 dye removal % is decreased.

As seen in Fig. 3, the percentage of chromium removal onto NACSW increased from 33% to a maximum of 72% in single removal and increased from 29% to a maximum of 59% in simultaneous pollutant removal when the pH was raised from 2 to 4, and at higher values of pH = 4, the removal decreases with increase in pH. Chromium(VI) in aqueous solution exists in one of three ionic forms: dichromate ion ($Cr_2O_7^{2-}$), hydrogen chromate ion ($HCrO_4^-$), and chromate ion (CrO_4^{2-}) [49]. At first, increasing initial pH values raises the concentration of $HCrO_4^-$ and CrO_4^{2-} and high electrostatic force of attraction between the negatively charged chromate ions and positively charged AC, the removal percentage of chromate increases [50]. At higher pH, the electrostatic repulsion between the negatively charged surface of the NACSW with the negatively charged Cr(VI) ions and competition between the excess OH^- and negative ion of Cr(VI), reduced the Cr(VI) adsorption capacity [50,51]. Solgi et al. [52] reported similar results for chromium removal in 2017 and Yahya et al. [53] reported the maximum removal efficiency for chromium at pH = 5.

Table 1
Main properties of the NACSW

Value	Unit	Parameter
962	m^2/g	Brunauer–Emmett–Teller
211.9	cm^3/g	V_m (monolayer volume)
9.62	nm	Mean pore diameter
741	–	BET constant *C*

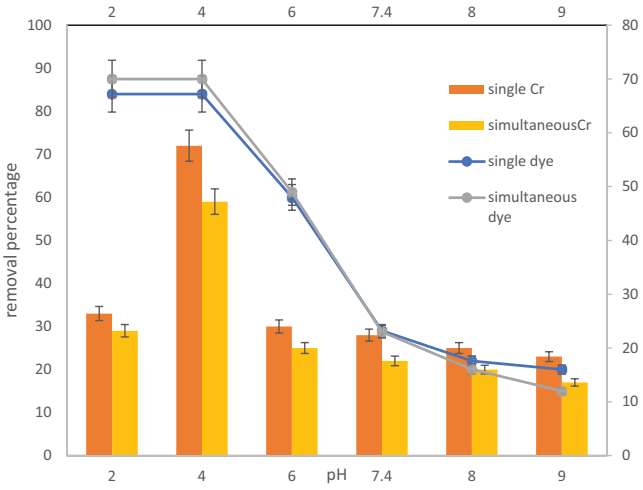

Fig. 3. Effect of solution pH 50 mL of 25 mg/L solutions of synthetic wastewater at 15 min.

3.2. Effect of adsorbent dosage

To optimize the adsorption process, the effect of dosage of adsorbent was investigated by changing the dosages of NACSW in the range of 0.10–0.50 g/L. The other parameters such as pollutants concentration (25 mg/L), initial pH (pH = 4), and time (15 min) were stable. In general, the adsorbent dosage of NACSW in single and simultaneous adsorption of Cr and RO P3R exerted a strong effect on the percentage removal (Fig. 4a). When the dosage of NACSW increased from 0.10 to 0.4 g/L, the percentage removal of dye increased from 42% to 84%, and Cr removal enhanced from 21% to 72% at single adsorption. Also, removal rates in simultaneous removal increased from 34% to 67% and 16% to 59% for dye and chromium, respectively (Fig. 4b). The removal efficiency of Cr and dye at single and simultaneous adsorption could be related to the increase in adsorbent mass or the vacant sites for adsorption [54]. However, further increases in the adsorbent dosage gave no major difference in the percentage removal of pollutants. It was probably due to the unsaturation of adsorption sites

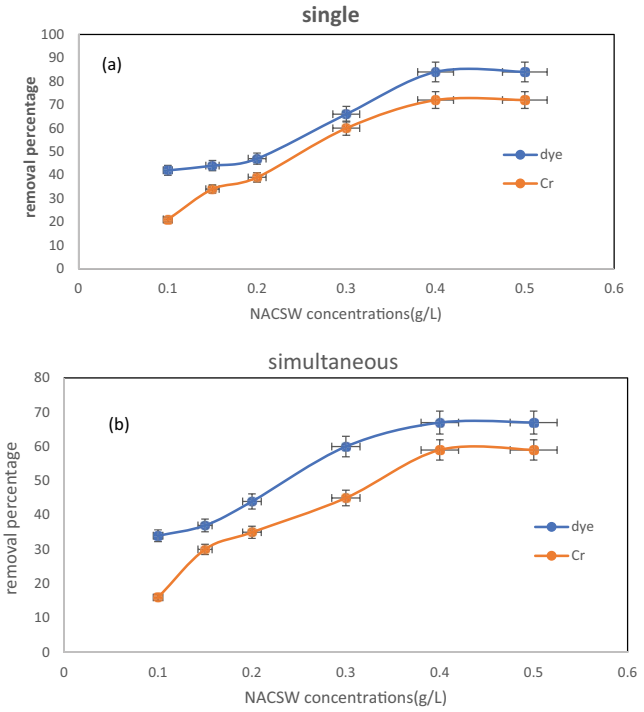

Fig. 4. Effect of various amounts of NACSW at 50 mL of 25 mg/L solution at pH = 4.0 at single (a) and simultaneous (b) state.

through the adsorption reaction [55]. These results are in accordance with what was reported by Mokhtari et al. [56] in the study of methyl orange removal.

3.3. Effect of contact time

In order to survey the contact time effect (2–40 min) on single and simultaneous removal efficiency of RO P3R and Cr, 0.04 g of NACSW per 100 mL aqueous solution at pH 4.0 was examined. Fig. 5 shows that in the first 15 min, the percentage of removal had a sharp rise and aftermath, the removal rate was approximately stable. Because at the initial stage, pollutants have access to many adsorption vacant sites [57]. Similar deductions and findings have been reported by Kumar et al. [58].

3.4. Mechanism associated with adsorption

The mechanisms of RO P3R and Cr removed by NACSW are proposed based on the above results. The FTIR spectra of NACSW within a range of 400–4,000 cm^{-1} analysis revealed the presence of a number of important functional groups. This is believed that carboxyl groups in aqueous solutions are ionized and removal occurs based on the electrostatic attraction between the activated carbons and Cr [59]. Also, free electron pairs derived from carboxyl or hydroxyl of NACSW surface groups can chelate the central chromium ion [59,60]. As the pH of the system increases, the removal decreases due to the competition of excess OH^- ions with anionic molecules of the pollutants for the adsorption sites and electrostatic repulsion [61].

3.5. Desorption and reusability

Reusability and stability are important factors in adsorbents. Reduction in the pollutants removal rate can be expected as the number of reuses is increased. Experiments were conducted to determine the efficacy of the reusability of NACSW. After adsorbing dye and chromium by NACSW, adsorbent efficiency was detected in the solution. The separated adsorbents are washed with deionized water and used for next adsorption cycle. As shown in Fig. 6, the adsorption amount of the adsorbent declined after six times of repeated use. the desorption and reusability efficiency of NACSW after six times can reach 49% (dye) and 40% (Cr), indicating that it has good efficiency.

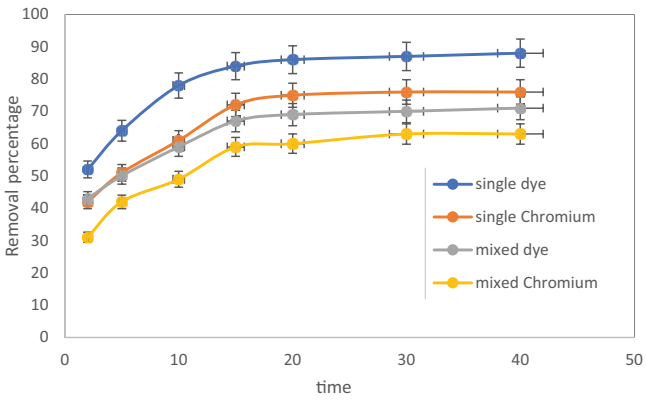

Fig. 5. Effect of contact time with 0.4 g/L of NACSW pH 4.0.

3.6. Adsorption kinetics study

Fig. 6 indicates single and simultaneous removal efficiency at different concentrations of Cr and RO P3R using adsorption onto NACSW as a function of contact time. Parameters of kinetics adsorption are useful for explaining the adsorption process and estimating the system up to industrial process scales. In this study, different kinetic models pseudo-first-order and pseudo-second-order, and Elovich reactions were investigated (Table 2). R^2 (correlation coefficients) from the Elovich kinetic model were higher than other kinetic models, implying that the single and simultaneous removal was better explained by Elovich. Rafati et al. [62] reported similar results in naproxen onto functionalized nano-clay composite adsorbent.

3.7. Isotherm modeling

Fig. 7 shows the adsorption isotherm of Reactive Orange P3R and chromium onto NACSW. As shown at lower concentration removal percentages of both pollutants separately and simultaneously was more. However, by increasing concentration, adsorption capacities are high due to the abundance number of pollutant molecules in solution and competition between pollutant-adsorbent interaction. The adsorption capacity increased until the sites are fully occupied and equilibrium is achieved. Table 3 shows the adsorption capacities of Cr and dye of the other sorbents reported in the previous literatures. Generally, activated carbon prepared from sycamore wood showed high Cr and dye removal efficiencies [63–67]. Table 4 summarizes information on the isotherm analysis and based on data the regression values of the Temkin isotherm were higher than those of the other isotherms. This indicates the applicability of Temkin isotherm in explaining the adsorption of chromium and dye in single and simultaneous state. In another study,

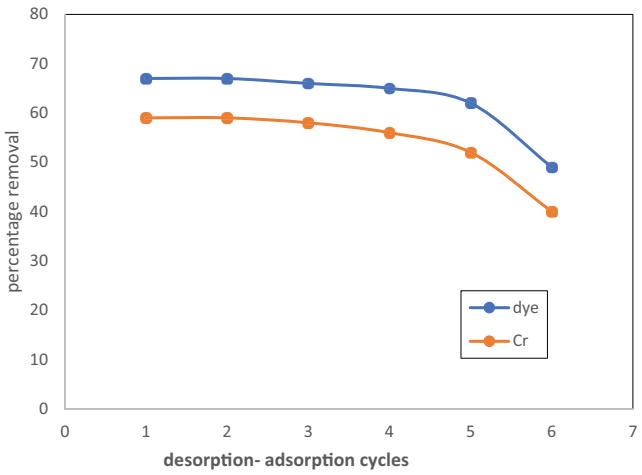

Fig. 6. Removal efficiency of Cr and dye with the recycled and regenerated NACSW (NACSW dosage: 0.4 g/L, pollutant concentration: 25 mg/L, initial pH: 4).

Table 2
Kinetic information of pollutants onto NACSW in single and simultaneous state

Elovich model			Pseudo-second-order			Pseudo-first-order			Effect of reaction kinetics
Separate dye	Separate chromium	Mixed dye	Mixed chromium	Separate dye	Separate chromium	Mixed dye	Mixed chromium	Separate dye	Separate chromium	Mixed dye	Mixed chromium	
$R^2 = 1.00$	$R^2 = 1.00$	$R^2 = 1.00$	$R^2 = 1.00$	$R^2 = 1.000$	$R^2 = 0.996$	$R^2 = 0.996$	$R^2 = 1.000$	$R^2 = 0.995$	$R^2 = 0.996$	$R^2 = 0.996$	$R^2 = 0.994$	
$\beta = 0.44$	$\beta = 0.42$	$\beta = 0.37$	$\beta = 0.36$	$q_e = 19.30$	$q_e = 21.28$	$q_e = 22.69$	$q_e = 24.81$	$q_e = 17.59$	$q_e = 19.88$	$q_e = 21.09$	$q_e = 23.20$	10 mg/L
$\alpha = 269$	$\alpha = 506$	$\alpha = 336$	$\alpha = 554$	$k_2 = 0.034$	$k_2 = 0.04$	$k_2 = 0.03$	$k_2 = 0.03$	$k_1 = 0.50$	$k_1 = 0.53$	$k_1 = 0.50$	$k_1 = 0.050$	
$R^2 = 0.99$	$R^2 = 1$	$R^2 = 1.000$	$R^2 = 1.00$	$R^2 = 0.996$	$R^2 = 0.998$	$R^2 = 0.997$	$R^2 = 0.998$	$R^2 = 0.994$	$R^2 = 0.997$	$R^2 = 0.996$	$R^2 = 0.997$	
$\beta = 0.13$	$\beta = 0.15$	$\beta = 0.12$	$\beta = 0.12$	$q_e = 42.23$	$q_e = 45.95$	$q_e = 50.48$	$q_e = 57.36$	$q_e = 37.73$	$q_e = 42.06$	$q_e = 45.66$	$q_e = 52.58$	25 mg/L
$\alpha = 53$	$\alpha = 193$	$\alpha = 101$	$\alpha = 269$	$k_2 = 0.008$	$k_2 = 0.01$	$k_2 = 0.01$	$k_2 = 0.01$	$k_1 = 0.26$	$k_1 = 0.38$	$k_1 = 0.30$	$k_1 = 0.37$	
$R^2 = 1.000$	$R^2 = 1$	$R^2 = 1.000$	$R^2 = 1.000$	$R^2 = 0.997$	$R^2 = 0.998$	$R^2 = 1.00$	$R^2 = 0.998$	$R^2 = 0.994$	$R^2 = 0.997$	$R^2 = 0.997$	$R^2 = 0.998$	
$\beta = 0.077$	$\beta = 0.07$	$\beta = 0.075$	$\beta = 0.071$	$q_e = 68,65$	$q_e = 75.87$	$q_e = 77,26$	$q_e = 96.20$	$q_e = 60.58$	$q_e = 67.76$	$q_e = 69.07$	$q_e = 87.77$	50 mg/L
$\alpha = 55$	$\alpha = 85$	$\alpha = 96$	$\alpha = 336$	$k_2 = 0.004$	$k_2 = 0.004$	$k_2 = 0.004$	$k_2 = 0.006$	$k_1 = 0.22$	$k_1 = 0.246$	$k_1 = 0.25$	$k_1 = 0.36$	

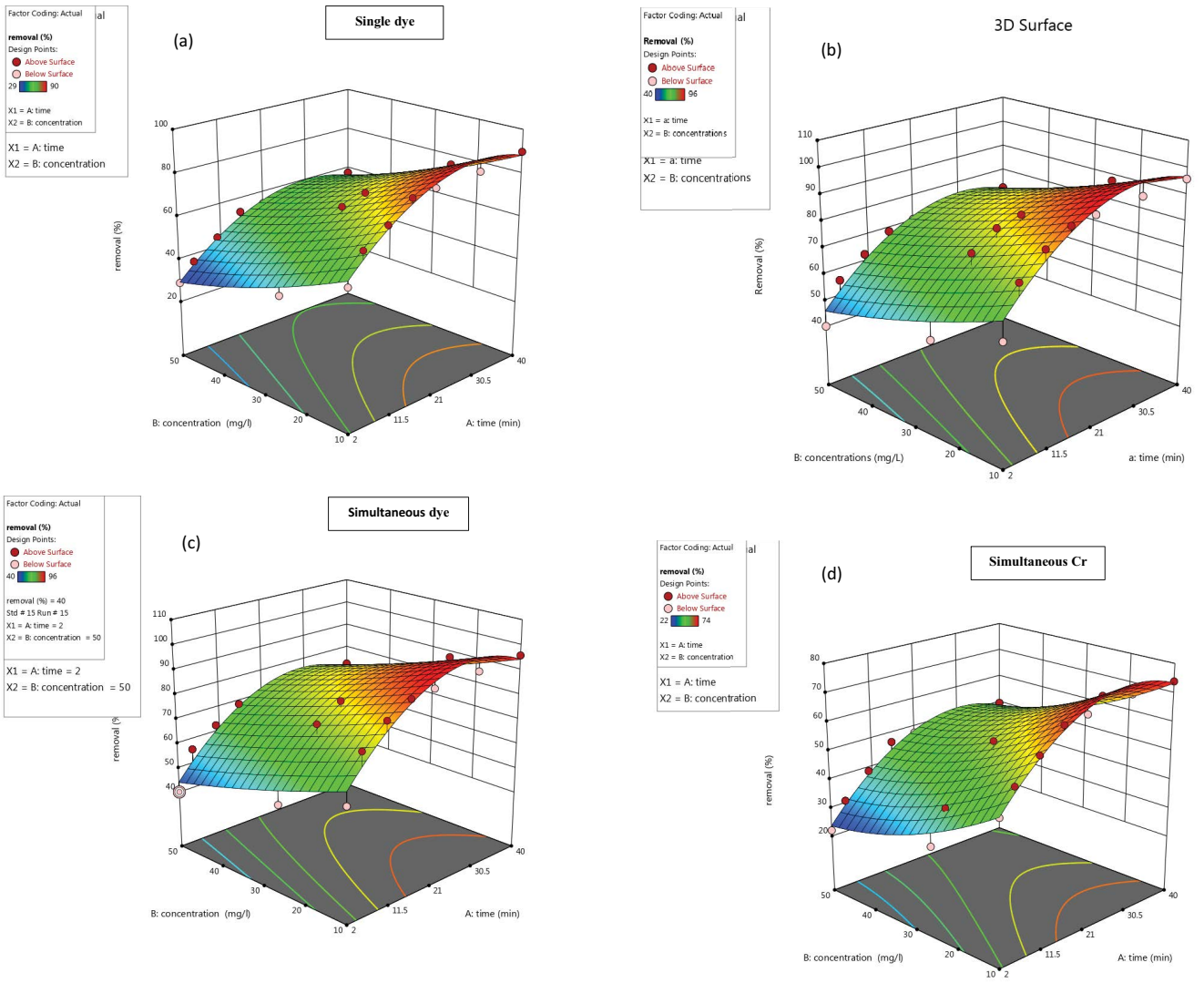

Fig. 7. Adsorption of various concentrations of single dye (a) and separate Cr (b) simultaneous dye (c) and simultaneous Cr and (d) state (10–50 mg/L) onto NACSW.

Table 3
Comparison of adsorption capacities for Cr and removal with other adsorbents

Adsorbent	Pollutant	Maximal adsorption capacity (mg/g)	References
NACSW	Cr	476.19	This study
Hazelnut shell activated carbon	Cr(VI)	170	[63]
Biochar-copolymer composite	Cr(VI)	491.3	[64]
Polypyrrole modified-$ZrPO_4$	Cr(VI)	62.5	[65]
NACSW	Reactive Orange P3R	588.24	This study
ZnO-activated carbon	Orange G	153.8	[66]
ZnO-activated carbons	Rhodamine B	128.2	[66]
Activated carbon	Methylene blue	615	[67]
Activated carbon	Congo red	339	[67]

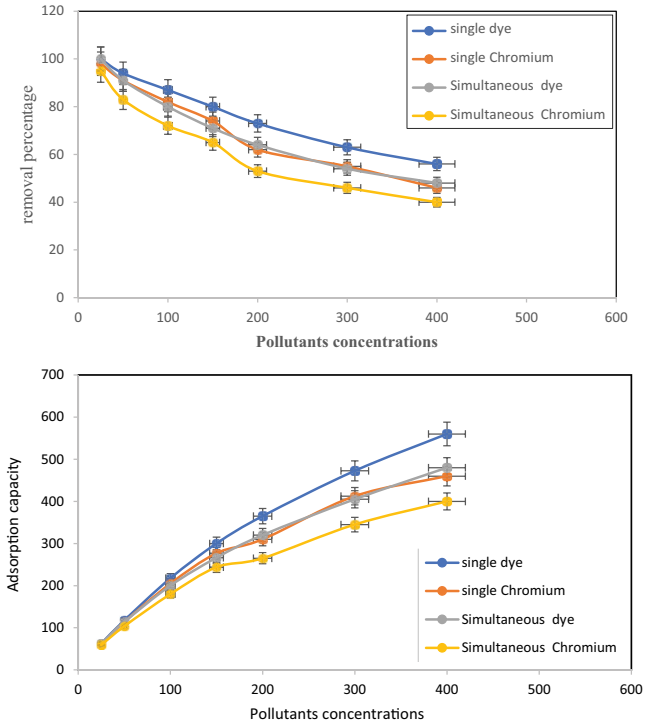

Fig. 8. Adsorption percentage (a) and capacity (b) of various concentrations of pollutants (50–400 mg/L) onto NACSW in single and simultaneous state under equilibrium condition.

Mohamed et al. [68] reported similar behavior in removing Cd^{2+} and Cr^{3+} ions by RPG.

4. Conclusions

In this study, the removal of Reactive Orange P3R (dye) and chromium (heavy metal) on synthesized activated carbon from sycamore wood was investigated in single and binary solutions. The prepared activated carbon has porous structure, high specific surface areas, and excellent adsorption performances. The results exhibited that the optimum conditions for removing ROP 3R and Cr were obtained at solution pH 4. Isotherm studies indicated that the Temkin model is best describes the process of both pollutants studied. The sorption kinetics of chromium and dye is more compatible with the Elovich model. The compare of removal rates in single and simultaneous states signified the locations of dye and chromium adsorption on NACSW are different.

References

[1] L. Cai, D. Ying, X. Liang, M. Zhu, X. Lin, Q. Xu, Z. Cai, X. Xu, N. Na, A novel cationic polyelectrolyte microsphere for ultrafast and ultra-efficient removal of heavy metal ions and dyes, Chem. Eng. J., 410 (2021) 128404, doi: 10.1016/j.cej.2021.128404.

[2] F.S.A. Khan, N.M. Mubarak, Y.H. Tan, M. Khalid, R.R. Karri, R. Walvekar, E.C. Abdullah, S. Nizamuddin, S.A. Mazari, A comprehensive review on magnetic carbon nanotubes and carbon nanotube-based buckypaper for removal of heavy metals and dyes, J. Hazard. Mater., 413 (2021) 125375, doi: 10.1016/j.jhazmat.2021.125375.

[3] I. Kariim, A.S. Abdulkareem, J.O. Tijani, O.K. Abubakre, Development of MWCNTs/TiO_2 nanoadsorbent for simultaneous removal of phenol and cyanide from refinery wastewater, Sci. Afr., 10 (2020) e00593, doi: 10.1016/j.sciaf.2020.e00593.

[4] M. Chen, R. Bi, R. Zhang, F. Yang, F. Chen, Tunable surface charge and hydrophilicity of sodium polyacrylate intercalated layered double hydroxide for efficient removal of dyes and heavy metal ions, Colloids Surf., A, 617 (2021) 126384, doi: 10.1016/j.colsurfa.2021.126384.

[5] J. Feng, S. Xiong, L. Ren, Y. Wang, Atomic layer deposition of TiO_2 on carbon-nanotubes membrane for capacitive deionization removal of chromium from water, Chin. J. Chem. Eng., 45 (2022) 15–21.

[6] H.-T. Hsu, S.-S. Chen, Y.-S. Chen, Removal of chromium(VI) and naphthalenesulfonate from textile wastewater by photocatalysis combining ionic exchange membrane processes, Sep. Purif. Technol., 80 (2011) 663–669.

[7] S.S. Kerur, S. Bandekar, M.S. Hanagadakar, S.S. Nandi, G.M. Ratnamala, P.G. Hegde, Removal of hexavalent chromium-industry treated water and wastewater: a review, Mater. Today Proc., 42 (2021) 1112–1121.

[8] X. Ren, S. Wang, Y. Jin, D. Xu, H. Yin, Adsorption properties of reactive dyes on the activated carbon from corn straw prepared by microwave pyrolysis, Desal. Water Treat., 200 (2020) 296–303.

[9] S. Ayuba, A.A. Mohammadib, M. Yousefic, F. Changanic, Performance evaluation of agro-based adsorbents for the removal of cadmium from wastewater, Desal. Water Treat., 142 (2019) 293–299.

[10] M. Gaikwad, C. Balomajumder, Removal of Cr(VI) and fluoride by membrane capacitive deionization with nanoporous and microporous *Limonia acidissima* (wood apple) shell activated carbon electrode, Sep. Purif. Technol., 195 (2018) 305–313.

[11] S. Lal, A. Singhal, P. Kumari, Exploring carbonaceous nanomaterials for arsenic and chromium removal from wastewater, J. Water Process Eng., 36 (2020) 101276, doi: 10.1016/j.jwpe.2020.101276.

[12] Y. Zhao, L. Li, Y. Zuo, G. He, Q. Chen, Q. Meng, H. Chen, Reduced graphene oxide supported ZnO/CdS heterojunction enhances photocatalytic removal efficiency of hexavalent chromium from aqueous solution, Chemosphere, 286 (2022) 131738, doi: 10.1016/j.chemosphere.2021.131738.

[13] A. Othmani, S. Magdouli, P. Senthil Kumar, A. Kapoor, P.V. Chellam, Ö. Gökkuş, Agricultural waste materials for adsorptive removal of phenols, chromium(VI) and cadmium(II) from wastewater: a review, Environ. Res., 204 (2022) 111916, doi: 10.1016/j.envres.2021.111916.

[14] D. Huang, C. Liu, C. Zhang, R. Deng, R. Wang, W. Xue, H. Luo, G. Zeng, Q. Zhang, X. Guo, Cr(VI) removal from aqueous solution using biochar modified with Mg/Al-layered double hydroxide intercalated with ethylenediaminetetraacetic acid, Bioresour. Technol., 276 (2019) 127–132.

[15] B. Thangagiri, A. Sakthivel, K. Jeyasubramanian, S. Seenivasan, J. Dhaveethu Raja, K. Yun, Removal of hexavalent chromium by biochar derived from *Azadirachta indica* leaves: batch and column studies, Chemosphere, 286 (2022) 131598, doi: 10.1016/j.chemosphere.2021.131598.

[16] C. Zhang, K. Cai, Q. Feng, Y. Xu, Z. Zhang, Chromium(VI) promotes cell migration through targeting epithelial-mesenchymal transition in prostate cancer, Toxicol. Lett., 300 (2019) 10–17.

[17] G.D. Değermenci, N. Değermenci, V. Ayvaoğlu, E. Durmaz, D. Çakır, E. Akan, Adsorption of reactive dyes on lignocellulosic waste; characterization, equilibrium, kinetic and thermodynamic studies, J. Cleaner Prod., 225 (2019) 1220–1229.

[18] A.H. Jawad, R.A. Rashid, M.A.M. Ishak, L.D. Wilson, Adsorption of methylene blue onto activated carbon developed from biomass waste by H_2SO_4 activation: kinetic, equilibrium and thermodynamic studies, Desal. Water Treat., 57 (2016) 25194–25206.

[19] Y. Rashtbari, S. Afshin, A. Hamzezadeh, M. Abazari, Y. Poureshgh, M. Fazlzadeh, Application of powdered activated

carbon coated with zinc oxide nanoparticles prepared using a green synthesis in removal of Reactive Blue 19 and Reactive Black-5: adsorption isotherm and kinetic models, Desal. Water Treat., 179 (2020) 354–367.
[20] M.L. Parisi, E. Fatarella, D. Spinelli, R. Pogni, R. Basosi, Environmental impact assessment of an eco-efficient production for coloured textiles, J. Cleaner Prod., 108 (2015) 514–524.
[21] S.C.M. Signorelli, J.M. Costa, A.F. de Almeida Neto, Electrocoagulation-flotation for orange II dye removal: kinetics, costs, and process variables effects, J. Environ. Chem. Eng., 9 (2021) 106157, doi: 10.1016/j.jece.2021.106157.
[22] K.Y. Foo, B.H. Hameed, An overview of dye removal via activated carbon adsorption process, Desal. Water Treat., 19 (2010) 255–274.
[23] M. Uygun, V. de la Asunción-Nadal, S. Evli, D.A. Uygun, B. Jurado-Sánchez, A. Escarpa, Dye removal by laccase-functionalized micromotors, Appl. Mater. Today, 23 (2021) 101045, doi: 10.1016/j.apmt.2021.101045.
[24] J. Cai, D. Zhang, W. Xu, W.-P. Ding, Z.-Z. Zhu, J.-R. He, S.-Y. Cheng, Polysaccharide-based hydrogels derived from cellulose: the architecture change from nanofibers to hydrogels for a putative dual function in dye wastewater treatment, J. Agric. Food Chem., 68 (2020) 9725–9732.
[25] S. Samsami, M. Mohamadizaniani, M.-H. Sarrafzadeh, E.R. Rene, M. Firoozbahr, Recent advances in the treatment of dye-containing wastewater from textile industries: overview and perspectives, Process Saf. Environ. Prot., 143 (2020) 138–163.
[26] E. Misran, O. Bani, E.M. Situmeang, A.S. Purba, Removal efficiency of methylene blue using activated carbon from waste banana stem: study on pH influence, IOP Conf. Ser.: Earth Environ. Sci., 122 (2018) 012085, doi: 10.1088/1755-1315/122/1/012085.
[27] S. Saito, Y. Matsui, Y. Yamamoto, S. Matsushita, S. Mima, N. Shirasaki, T. Matsushita, Oxidative removal of soluble divalent manganese ion by chlorine in the presence of superfine powdered activated carbon, Water Res., 187 (2020) 116412, doi: 10.1016/j.watres.2020.116412.
[28] H. Shi, Q. Wang, J. Ni, Y. Xu, N. Song, M. Gao, Highly efficient removal of amoxicillin from water by three-dimensional electrode system within granular activated carbon as particle electrode, J. Water Process Eng., 38 (2020) 101656, doi: 10.1016/j.jwpe.2020.101656.
[29] M.A. Hashim, A. Kundu, S. Mukherjee, Y.-S. Ng, S. Mukhopadhyay, G. Redzwan, B. Sen Gupta, Arsenic removal by adsorption on activated carbon in a rotating packed bed, J. Water Process Eng., 30 (2019) 100591, doi: 10.1016/j.jwpe.2018.03.006.
[30] M.A. Al-Ghouti, A.O. Sweleh, Optimizing textile dye removal by activated carbon prepared from olive stones, Environ. Technol. Innovation, 16 (2019) 100488, doi: 10.1016/j.eti.2019.100488.
[31] C. Arora, P. Kumar, S. Soni, J. Mittal, A. Mittal, B. Singh, Efficient removal of malachite green dye from aqueous solution using *Curcuma caesia* based activated carbon, Desal. Water Treat., 195 (2020) 341–352.
[32] J. Wang, C. Chen, Chitosan-based biosorbents: modification and application for biosorption of heavy metals and radionuclides, Bioresour. Technol., 160 (2014) 129–141.
[33] A. Alahabadi, P. Singh, P. Raizada, I. Anastopoulos, S. Sivamani, G.L. Dotto, M. Landarani, A. Ivanets, G.Z. Kyzas, A. Hosseini-Bandegharaei, Activated carbon from wood wastes for the removal of uranium and thorium ions through modification with mineral acid, Colloids Surf., A, 607 (2020) 125516, doi: 10.1016/j.colsurfa.2020.125516.
[34] J. Jin, S. Li, X. Peng, W. Liu, C. Zhang, Y. Yang, L. Han, Z. Du, K. Sun, X. Wang, HNO_3 modified biochars for uranium(VI) removal from aqueous solution, Bioresour. Technol., 256 (2018) 247–253.
[35] L. Dolatyari, M.R. Yaftian, S. Rostamnia, Removal of uranium(VI) ions from aqueous solutions using Schiff base functionalized SBA-15 mesoporous silica materials, J. Environ. Manage., 169 (2016) 8–17.
[36] Y. Sun, Y. Gu, P. Zhang, Adsorption properties and recognition mechanisms of a novel surface imprinted polymer for selective removal of Cu(II)-citrate complexes, J. Hazard. Mater., 424 (2022) 127735, doi: 10.1016/j.jhazmat.2021.127735.
[37] K.G. Akpomie, J. Conradie, Advances in application of cotton-based adsorbents for heavy metals trapping, surface modifications and future perspectives, Ecotoxicol. Environ. Saf., 201 (2020) 110825, doi: 10.1016/j.ecoenv.2020.110825.
[38] T.C. Egbosiuba, A.S. Abdulkareem, A.S. Kovo, E.A. Afolabi, J.O. Tijani, M. Auta, W.D. Roos, Ultrasonic enhanced adsorption of methylene blue onto the optimized surface area of activated carbon: adsorption isotherm, kinetics and thermodynamics, Chem. Eng. Res. Des., 153 (2020) 315–336.
[39] J. Kluczka, W. Pudło, K. Krukiewicz, Boron adsorption removal by commercial and modified activated carbons, Chem. Eng. Res. Des., 147 (2019) 30–42.
[40] F. Riahimanesh, A. Alahabadi, M. Baghayeri, B. Maleki, M. Miri, Investigation on the removal of entacapone from contaminated water using magnetic activated carbon, Mater. Res. Express, 6 (2019) 096105, doi: 10.1088/2053-1591/ab2ceb.
[41] N.S.M. Desa, Z.A. Ghani, S.A. Talib, C.C. Tay, Performance of spent mushroom farming waste (SMFW) activated carbon for Ni(II) removal, IOP Conf. Ser.: Mater. Sci. Eng., 136 (2016) 012059, doi: 10.1088/1757-899X/136/1/012059.
[42] T. Ahmad, M. Danish, Prospects of banana waste utilization in wastewater treatment: a review, J. Environ. Manage., 206 (2018) 330–348.
[43] G. Moussavi, A. Alahabadi, K. Yaghmaeian, M. Eskandari, Preparation, characterization and adsorption potential of the NH_4Cl-induced activated carbon for the removal of amoxicillin antibiotic from water, Chem. Eng. J., 217 (2013) 119–128.
[44] C. Jiang, G.A. Yakaboylu, T. Yumak, J.W. Zondlo, E.M. Sabolsky, J. Wang, Activated carbons prepared by indirect and direct CO_2 activation of lignocellulosic biomass for supercapacitor electrodes, Renewable Energy, 155 (2020) 38–52.
[45] N.N.A. Malek, A.H. Jawad, K. Ismail, R. Razuan, Z.A. Alothman, Fly ash modified magnetic chitosan-polyvinyl alcohol blend for Reactive Orange 16 dye removal: adsorption parametric optimization, Int. J. Biol. Macromol., 189 (2021) 464–476.
[46] T. Calvete, E.C. Lima, N.F. Cardoso, J.C.P. Vaghetti, S.L.P. Dias, F.A. Pavan, Application of carbon adsorbents prepared from Brazilian-pine fruit shell for the removal of Reactive Orange 16 from aqueous solution: kinetic, equilibrium, and thermodynamic studies, J. Environ. Manage., 91 (2010) 1695–1706.
[47] A.S. Abdulhameed, A.-T. Mohammad, A.H. Jawad, Application of response surface methodology for enhanced synthesis of chitosan tripolyphosphate/TiO_2 nanocomposite and adsorption of Reactive Orange 16 dye, J. Cleaner Prod., 232 (2019) 43–56.
[48] D.D. Eslek Koyuncu, M. Okur, Removal of AV 90 dye using ordered mesoporous carbon materials prepared via nanocasting of KIT-6: adsorption isotherms, kinetics and thermodynamic analysis, Sep. Purif. Technol., 257 (2021) 117657, doi: 10.1016/j.seppur.2020.117657.
[49] B. Tu, R. Wen, K. Wang, Y. Cheng, Y. Deng, W. Cao, K. Zhang, H. Tao, Efficient removal of aqueous hexavalent chromium by activated carbon derived from Bermuda grass, J. Colloid Interface Sci., 560 (2020) 649–658.
[50] W. Wang, Chromium(VI) removal from aqueous solutions through powdered activated carbon counter-current two-stage adsorption, Chemosphere, 190 (2018) 97–102.
[51] M. Su, Y. Fang, B. Li, W. Yin, J. Gu, H. Liang, P. Li, J. Wu, Enhanced hexavalent chromium removal by activated carbon modified with micro-sized goethite using a facile impregnation method, Sci. Total Environ., 647 (2019) 47–56.
[52] M. Solgi, T. Najib, S. Ahmadnejad, B. Nasernejad, Synthesis and characterization of novel activated carbon from Medlar seed for chromium removal: experimental analysis and modeling with artificial neural network and support vector regression, Resour.-Effic. Technol., 3 (2017) 236–248.
[53] M.D. Yahya, K.S. Obayomi, M.B. Abdulkadir, Y.A. Iyaka, A.G. Olugbenga, Characterization of cobalt ferrite-supported activated carbon for removal of chromium and lead ions from

tannery wastewater via adsorption equilibrium, Water Sci. Eng., 13 (2020) 202–213.
[54] D. Anitha, A. Ramadevi, R. Seetharaman, Activated Mangosteen shell in removal of mercury ion from aqueous solution, Mater. Today: Proc., 45 (2021) 658–662.
[55] R. Zakaria, N.A. Jamalluddin, M.Z. Abu Bakar, Effect of impregnation ratio and activation temperature on the yield and adsorption performance of mangrove based activated carbon for methylene blue removal, Results Mater., 10 (2021) 100183, doi: 10.1016/j.rinma.2021.100183.
[56] P. Mokhtari, M. Ghaedi, K. Dashtian, M.R. Rahimi, M.K. Purkait, Removal of methyl orange by copper sulfide nanoparticles loaded activated carbon: kinetic and isotherm investigation, J. Mol. Liq., 219 (2016) 299–305.
[57] A. Rahmani-Sani, P. Singh, P. Raizada, E. Claudio Lima, I. Anastopoulos, D.A. Giannakoudakis, S. Sivamani, T.A. Dontsova, A. Hosseini-Bandegharaei, Use of chicken feather and eggshell to synthesize a novel magnetized activated carbon for sorption of heavy metal ions, Bioresour. Technol., 297 (2020) 122452, doi: 10.1016/j.biortech.2019.122452.
[58] J.A. Kumar, P.S. Kumar, T. Krithiga, D. Prabu, D.J. Amarnath, S. Sathish, D. Venkatesan, A. Hosseini-Bandegharaei, P. Prashant, Acenaphthene adsorption onto ultrasonic assisted fatty acid mediated porous activated carbon-characterization, isotherm and kinetic studies, Chemosphere, 284 (2021) 131249, doi: 10.1016/j.chemosphere.2021.131249.
[59] B. Kaźmierczak, J. Molenda, M. Swat, The adsorption of chromium(III) ions from water solutions on biocarbons obtained from plant waste, Environ. Technol. Innovation, 23 (2021) 101737, doi: 10.1016/j.eti.2021.101737.
[60] K. Henryk, C. Jarosław, Ż. Witold, Peat and coconut fiber as biofilters for chromium adsorption from contaminated wastewaters, Environ. Sci. Pollut. Res., 23 (2016) 527–534.
[61] F.R. Furlan, L.G. de Melo da Silva, A.F. Morgado, A.A.U. de Souza, S.M.A. Guelli Ulson de Souza, Removal of reactive dyes from aqueous solutions using combined coagulation/flocculation and adsorption on activated carbon, Resour. Conserv. Recycl., 54 (2010) 283–290.
[62] L. Rafati, M.H. Ehrampoush, A.A. Rafati, M. Mokhtari, A.H. Mahvi, Modeling of adsorption kinetic and equilibrium isotherms of naproxen onto functionalized nano-clay composite adsorbent, J. Mol. Liq., 224 (2016) 832–841.
[63] C. Zwiener, F.H. Frimmel, Oxidative treatment of pharmaceuticals in water, Water Res., 34 (2000) 1881–1885.
[64] J. Deng, Y. Liu, H. Li, Z. Huang, X. Qin, J. Huang, X. Zhang, X. Li, Q. Lu, A novel biochar-copolymer composite for rapid Cr(VI) removal: adsorption-reduction performance and mechanism, Sep. Purif. Technol., 295 (2022) 121275, doi: 10.1016/j.seppur.2022.121275.
[65] A. Behera, S. Sahu, S. Pahi, S.K. Singh, B. Mahapatra, R.K. Patel, Polypyrrole modified zirconium(IV) phosphate nanocomposite: an effective adsorbent for Cr(VI) removal by adsorption-reduction mechanism, Mater. Chem. Phys., 290 (2022) 126540, doi: 10.1016/j.matchemphys.2022.126540.
[66] J. Saini, V.K. Garg, R.K. Gupta, N. Kataria, Removal of Orange G and Rhodamine B dyes from aqueous system using hydrothermally synthesized zinc oxide loaded activated carbon (ZnO-AC), J. Environ. Chem. Eng., 5 (2017) 884–892.
[67] F. Amran, M.A.A. Zaini, Valorization of *Casuarina* empty fruit-based activated carbons for dyes removal – activators, isotherm, kinetics and thermodynamics, Surf. Interfaces, 25 (2021) 101277, doi: 10.1016/j.surfin.2021.101277.
[68] H.S. Mohamed, N.K. Soliman, D.A. Abdelrheem, A.A. Ramadan, A.H. Elghandour, S.A. Ahmed, Adsorption of Cd^{2+} and Cr^{3+} ions from aqueous solutions by using residue of *Padina gymnospora* waste as promising low-cost adsorbent, Heliyon, 5 (2019) e01287, doi: 10.1016/j.heliyon.2019.e01287.